Late Triassic detrital zircons in meta-turbidites of the Chonos Metamorphic Complex, southern Chile

Francisco Hervé

Departamento de Geología, Universidad de Chile, Casilla 13518, Correo 21, Santiago, Chile
fherve@cec.uchile.cl

C. Mark Fanning

Research School of Earth Sciences, The Australian National University, Canberra, ACT 0200, Australia

ABSTRACT

Sensitive High Resolution Ion MicroProbe (SHRIMP) U-Pb age determinations of detrital zircons from metasandstones of the Chonos Metamorphic Complex reveal a significant population of Late Triassic ages. One of the samples is immediately underlying the coquinaceous bed containing fossils which were initially identified as Late Silurian-Early Devonian, and more recently as Late Triassic faunas. The zircon data confirm the latter age as the depositional age of the fossil bearing rocks, excluding completely the possibility of a Paleozoic depositional age. Similar U-Pb detrital zircon ages are recorded in two other samples, one of which was collected in the vicinity of strata containing *Lima* sp., confirming that a Late Triassic depositional age is widespread in the Eastern belt of the Chonos Metamorphic Complex. However, in a fourth sample, the youngest detrital zircons are Carboniferous in age. Construction of the accretionary prism was thus active in the Late Triassic, and its metamorphism probably took place during the Jurassic, in contrast with a previously accepted Late Paleozoic age.

Key words: Late Triassic, U-Pb ages, Chonos Metamorphic Complex, Southern Chile.

RESUMEN

Circones detríticos del Triásico tardío en metaturbiditas del Complejo Metamórfico Chonos, sur de Chile. Las edades U-Pb de circones detríticos, obtenidas con el SHRIMP en metareniscas del Complejo Metamórfico de Chonos, revelan una abundante población de circones con edades correspondientes al Triásico Superior. Una de las muestras proviene del estrato que se ubica inmediatamente bajo la capa coquinácea con fósiles que inicialmente otros autores asignaron al Silúrico Superior-Devónico Inferior, y recientemente al Triásico Superior. Las edades de circones detríticos concuerdan totalmente con esta última, y eliminan la posibilidad de una edad paleozoica de deposición de las rocas fosilíferas. Otras dos muestras, una de las cuales proviene de las vecindades de un estrato que contiene *Lima* sp., dan resultados similares, lo que indica que esta edad de deposición tiene amplia distribución en la franja oriental del Complejo Metamórfico de los Chonos. En cambio, en una cuarta muestra la edad más joven de circones detríticos es carbonífera. La construcción del prisma de acreción estaba activa en el Triásico Superior, y su metamorfismo tuvo lugar, probablemente, durante el Jurásico, contrariamente a la edad paleozoica superior que se le asignaba hasta ahora.

Palabras claves: Triásico tardío, Edades U-Pb, Complejo Metamórfico Chonos, Sur de Chile.

Revista Geológica de Chile, Vol. 28, No. 1, p. 91-104, 4 Figs., 4 tables, July 2001.

INTRODUCTION

The Chonos Metamorphic Complex (CMC) is part of an accretionary complex which crops out as a continuous belt in the coastal area of Chile from Pichilemu (34°S) to the Taitao Peninsula (47°S), and discontinuously from there to the southernmost tip of South America.

The time frame proposed for the evolution of the low grade Chonos Metamorphic Complex (Davidson *et al.*, 1987), and for all the accretionary complex (*e.g.*, Hervé, 1988), has been strongly influenced by the identification by Miller and Sprechmann (1978) of a Late Silurian-Early Devonian fossil fauna in a coquinaceous metaturbidite bed in the southern end of Isla Patranca and in a small unnamed islet 5 km to the north. These fossiliferous localities, unique within the whole complex, were re-examined by Fang *et al.* (1998) who identified more recently collected fossil specimens as a Late Triassic *Monotis* species in Isla Patranca (named Potranca in Miller and Sprechmann, 1978) and *Lima* sp., of a Permian to Triassic age range.

The Chonos Metamorphic Complex has been studied previously by Miller (1979) and Hervé *et al.* (1981). Detailed field and structural studies led Miller (1979) to recognize three stratigraphic units, the Canal King, Potranca and Canal Pérez Sur informal formations, interpreted to be progressively younger successions, separated by unconformities. However, the three units share a common structural grain, characterized by northwest trending fold axes and stretching lineations. The fossil assemblages noted above occur in the middle Potranca formation, which was assigned to the Late Silurian-Early Devonian. It follows that the underlying Canal King formation is older and that the overlying Canal Pérez Sur formation is younger.

In an alternative view, Hervé *et al.* (1981) distinguishes an Eastern belt* where primary sedimentary structures are preserved, which grades into a Western belt where all primary structures have been lost due to increasing deformation and metamorphism. This interpretation is based on both structural continuity and a progressive increase in metamorphic grade from one belt to the other. The Eastern belt is considered to have a Devonian protholith, and be composed of the Patranca facies and the Teresa facies, roughly equivalent to the Potranca and Canal Pérez Sur formations of Miller (1979), respectively. Davidson *et al.* (1987) presented Rb-Sr whole rock ages of *ca.* 220 Ma on slates from the Eastern belt which were interpreted as the age of the D2 metamorphic episode in the complex. They presented Rb-Sr errorchron data on the schists from the Western belt of *ca.* 140 Ma and *ca.* 168 Ma which they interpreted as indicating a Jurassic 'reactivation' of the subduction complex.

Willner *et al.* (2000) have shown that the metamorphism within the Eastern belt of the Chonos Metamorphic Complex took place under peak P-T conditions of 5.5 Kbar and 250-280°C and 8-10 Kbar and 380-500°C in the Western belt. These rather high P-T gradients are in accordance with a subduction zone environment of metamorphism.

The purpose of this paper is to present the results of SHRIMP U-Pb age determinations for detrital zircons from rocks of the fossiliferous unit. These results elucidate the contradiction between the two previously published paleontological age interpretations and they establish constraints on the age of deposition and metamorphism of the Potranca formation in the Chonos Metamorphic Complex.

SAMPLES AND METHODOLOGY

Three metasedimentary rock samples of the turbiditic unit (Potranca formation or Patranca facies of the Eastern belt) which contain the fossiliferous strata in the Chonos Metamorphic Complex were collected for U-Th-Pb dating of zircon by SHRIMP (Sensitive High Resolution Ion MicroProbe) at The Australian National University. An additional metasedimentary rock from the Teresa facies (Ca-

* The terms Eastern and Western belts as used here should not be confused with the terms Western and Eastern Series, terminology that has been the formal nomenclature since Aguirre *et al.* (1972), used with the accretionary complex north of Chiloé and more recently by Martin *et al.* (1999), for rocks found between 38 and 41°S.

nal Pérez Sur formation) was also analysed. Zircons were separated using standard crushing, heavy liquid and Frantz isodynamic methods. Grains from the total zircon population were sprinkled onto double sided tape and cast in an epoxy disk together with the Duluth Gabbro reference zircon, AS3 (see Paces and Miller, 1993). The ion microprobe procedures used essentially follow those given in Compston *et al.* (1992) and Williams (1998). The U/Pb ratios have been calibrated relative to the AS3 zircons, which have an age of 1099 Ma (Paces and Miller, 1993).One spot was analyzed in each crystal, unless specified in the tables by a number of the form n.2, usually in the outer rim.

The age spectra of individual rock units can be used to obtain an inferred maximum depositional age of the original sediments; the depositional age can be no older than the youngest concordant U-Pb zircon age. Where a number of analyses (from different grains) have the same radiogenic $^{206}Pb/^{238}U$ ratios to within analytical uncertainty, weighted mean ages have been calculated and those are reported, with uncertainties given at the 95% confidence level.

All samples analysed belong to the Eastern Belt of the Chonos Metamorphic Complex. Their location is indicated in figure 1.

CE9603 is a metasandstone with L-tectonite fabric reflecting the intersection of two cleavages in northwest direction. It was collected from a turbidite succesion devoid of fossils.

FO9606 is a medium grained metasandstone with convolute bedding. It was collected near the southern end of Isla Patranca, from an horizon immediately underlying the coarse grained fossil bearing coquinaceous bed from which Miller and Sprechman (1978) and Fang *et al.* (1998) have identified Late Silurian-Early Devonian and Late Triassic fossils respectively. The coquinaceous bed from this location shows clear indications of having previously been sampled. The authors, therefore, believe that this coquinaceous bed was sampled to produce the Miller and Sprechman (1978) fossils, and the authors know with absolute certainty that this is the location described in Fang *et al.* (1998) since the material was collected by the senior author. The contact between the metasandstone sampled for this U-Pb zircon study and the coquinaceous bed used for the fossil age determinations is of normal conformable sedimentary nature.

CE9625 is a low grade fine grained metaconglomerate collected in the islet where *Lima* sp. was identified by Fang *et al.* (1998). Continuous slate beds form only 5% of the succesion, which is mainly composed here by turbidites with sole marks, dewatering structures, convolute bedding and rip clasts of shale. The rocks are cleaved and have a northwest lineation.

FO9640 is a fine grained metasandstone from the southeastern corner of Isla Yechica, where an inverted succession of turbidites with interbedded banded cherts crops out. Beds are typically 0.5 m thick, bioturbated, and with a subhorizontal tectonic lamination, axial planar to ENE folds of the stratification.

GEOCHRONOLOGICAL RESULTS

The SHRIMP U-Pb detrital zircon results for the samples CE9603, FO9606 and CE9625 (Patranca facies or Potranca formation) are presented in tables 1-4, p. 101-104 . The results for sample FO9640 (Teresa facies or Canal Pérez Sur formation) are presented in table 4. The data are shown on the Tera-Wasserburg diagrams in figure 2, and on relative probability plots in figure 3, respectively.

The three samples of the Potranca facies record similar results, with a wide range of ages. The age spectra are complex revealing multiple source provenance for the detrital zircon grains.

However, some common aspects between the samples can be highlighted:

- Most of the zircons are igneous in origin, they have euhedral to subhedral outlines and cathodoluminescence (CL) images of the sectioned grains show well developed, simple magmatic zoning.
- The youngest zircon analysis in each sample, with isotopic ratios plotting within uncertainty of the Tera-Wasserbug concordia, are *ca.* 210 Ma (212, 216 and 208 Ma, respectively). There are few analyses which are younger, however these are discordant and so the ages are not considered to

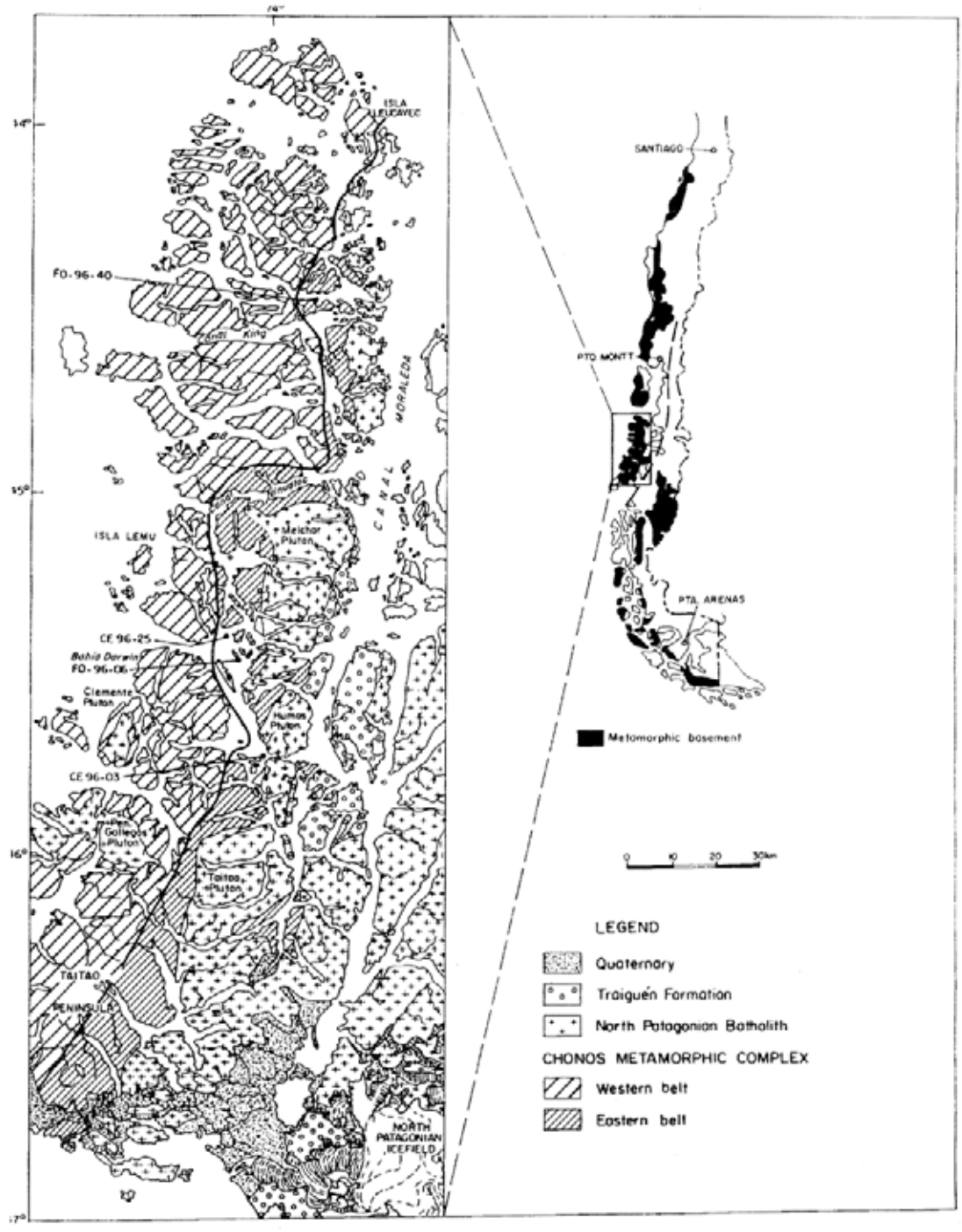

FIG. 1. Geologic sketch map of the Chonos Archipelago region, with indication of geologic units as in Davidson *et al.* (1987) and location of the analysed samples.

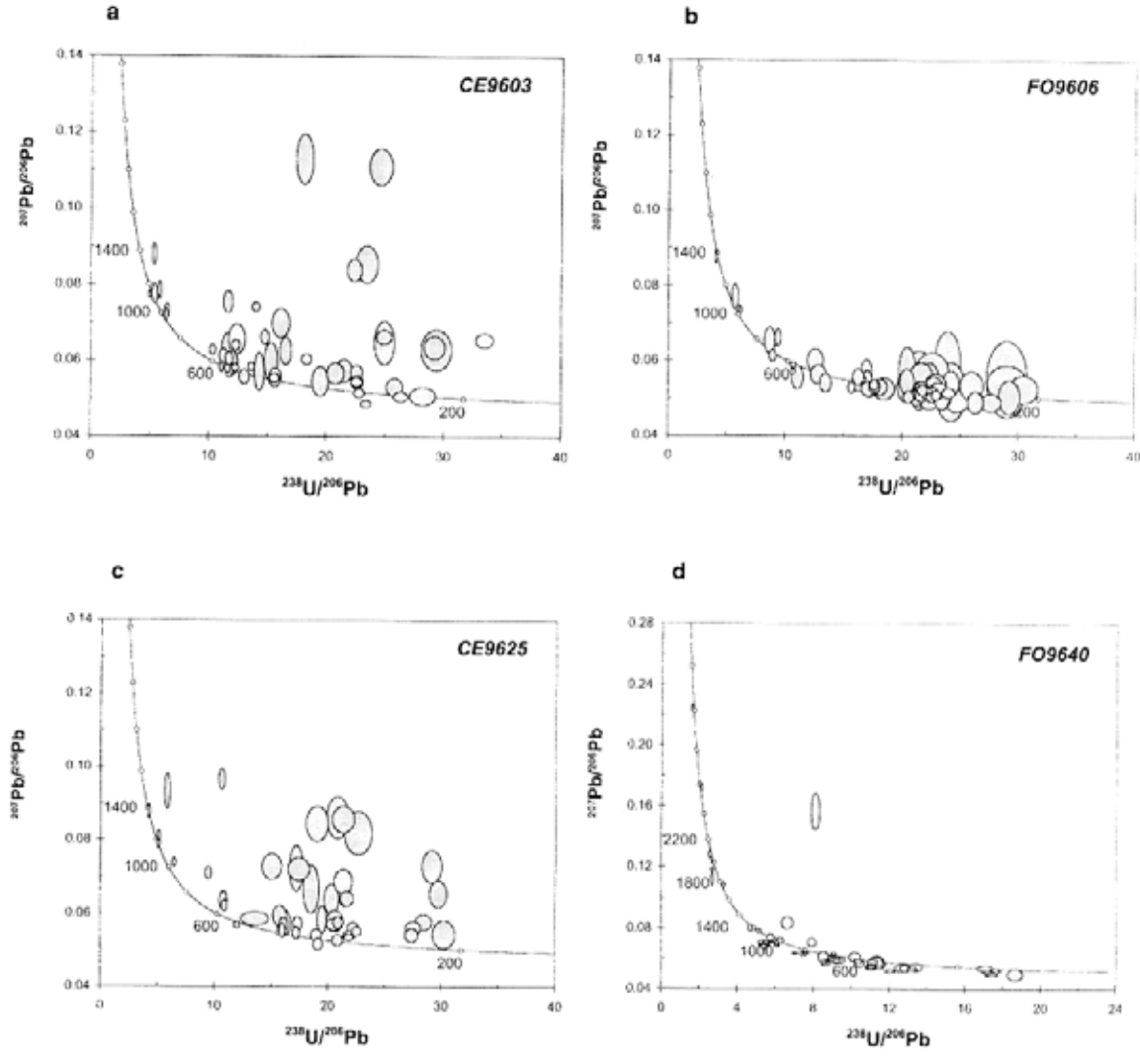

FIG. 2. Tera and Wasserburg (1972) concordia diagrams for **a-** sample CE9603; **b-** sample FO9606; **c-** sample CE9625, and **d-** sample CE9640. The calibrated $^{238}U/^{206}Pb$ ratios *versus* the total $^{207}Pb/^{206}Pb$ ratios have been plotted as one sigma error ellipses. Note that an analysis that is not within uncertainty of the concordia curve may not necessarily signify a discordant analysis. It may simply reflect that a significant amount of common Pb has been detected in that analysis. The U/Pb isotopic data are given in the tables as both uncorrected and ^{207}Pb corrected radiogenic ratios (see Compston *et al.*, 1992).

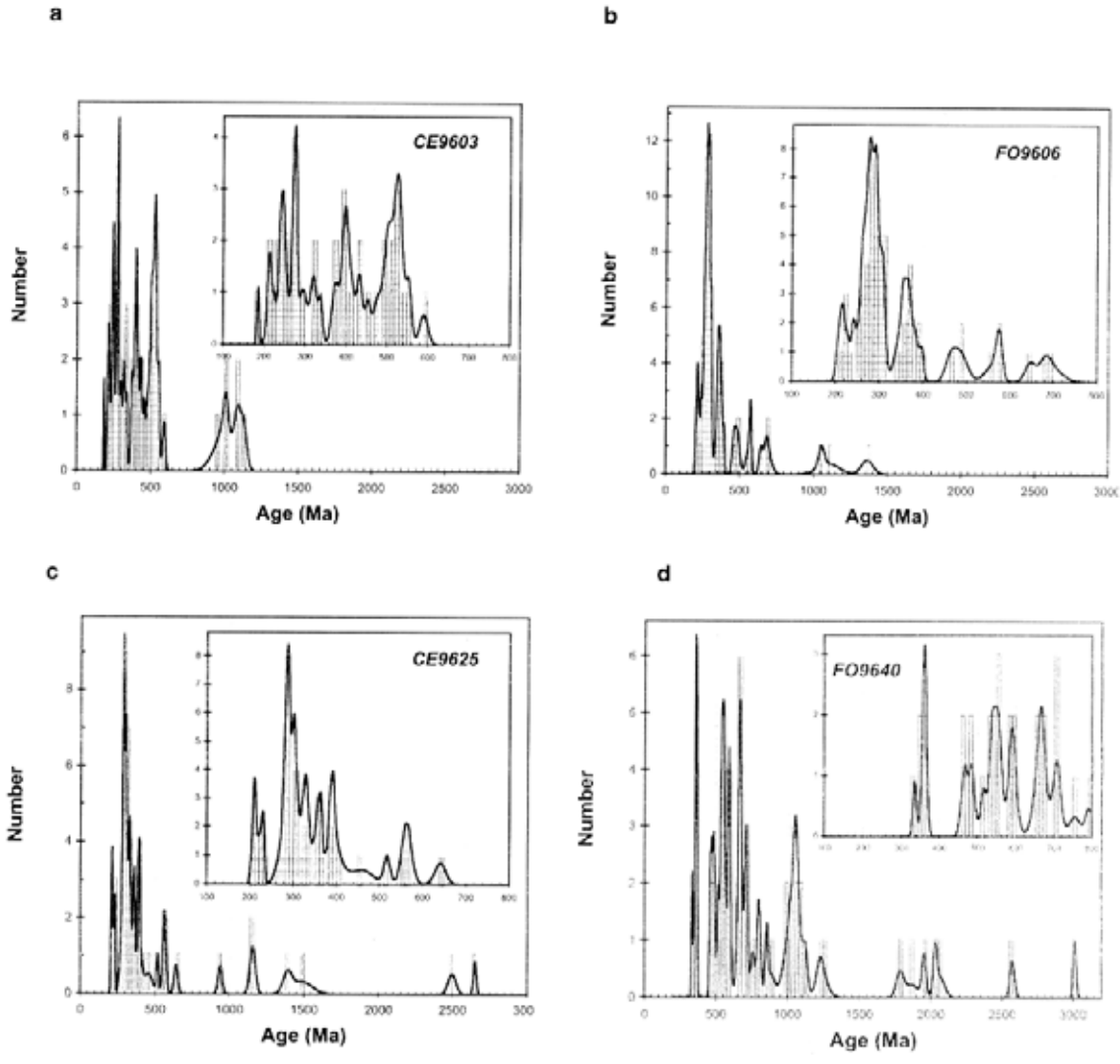

FIG. 3. Age *versus* probability diagrams for **a-** sample CE9603; **b-** sample FO9606; **c-** sample CE9625, and **d-** sample F09640. The relative probability curve takes into account the age and age uncertainty for each analysis. The stacked histogram indicates the number of analyses that contribute to the various peaks in the relative probability curve.

necessarily represent the time of crystallisation of the zircons. The youngest concordant ages form a grouping at *ca.* 220 Ma in all three samples.

- Most (>80%) of the zircons analysed are Paleozoic in age, and they show a complex distribution with age peaks (Figs. 1b, 2b, 3b) at *ca.* 280 Ma, at 330-350 Ma, at 400 Ma, with very few zircons between 400 and 530 Ma, and a further peak at *ca.* 550 Ma.
- Proterozoic zircons are scarce, they are mainly concentrated in the 1300-1600 Ma age range, and are absent at 800±50 Ma.
- Only two Late Archean and/or Paleoproterozoic zircons are present in one of the samples.

The results for sample F09640 (from the Teresa facies or Canal Pérez Sur formation) differ quite substantialy from the above. The younger datefor detrital zircons in this sample is 336±5 Ma (Early Carboniferous), and the proportion of Proterozoic grains is larger than in the three previous samples. Two Archean grains are present.

DISCUSSION AND CONCLUSIONS

The U-Pb SHRIMP zircon age data obtained in this study strongly support the Late Triassic (Late Norian) depositional age determination made by Fang *et al.* (1998) based on the study of fossils in the Chonos Metamorphic Complex, and is in contradiction with the previously proposed Late Silurian-Early Devonian age by Miller and Sprechmann (1978). The fact that three samples from the same unit (the Potranca ormation or Patranca facies) of the Chonos Metamorphic Complex show similar minimum ages indicates that the Late Triassic rocks are extensive and not simply restricted to the fossiliferous localities.

The coincidence between the radioisotopic zircon ages and the biostratigraphic depositional ages (Gradstein and Ogg, 1996) is remarkable, and probably indicates that active magmatism was ocurring in the provenance area of the turbidite sequence during their deposition.

This provenance area is almost instinctively looked for in Patagonia, to the east of the analysed samples. However, in the Chilean slope of the Andes, igneous rocks of Late Triassic age are not known. A few granitic bodies of Late Triassic age do exist in the North Patagonian Massif (Cingolani *et al.*, 1992), hundreds of kilometers inland from the location of the Chonos Archipelago. A Carboniferous magmatic arc in the Lake District of Chile, was exhumated and eroded previously to the Late Triassic (Martin, 1999). Also, the Mesoproterozoic and Late Proterozoic zircons, might have come from the presently covered basement of Patagonia, or they may be far travelled grains coming from the Namaquan belts of southern Africa, which was side by side to Patagonia in the Late Triassic.

Another possible source area for the detrital material is the Antarctic Peninsula (Fig. 4), whose exact position in the Early Mesozoic is not well known, but that in recent paleogeographic reconstructions, is located with its northern tip near the present latitude of the Golfo de Penas (47°S) (Lawver *et al.*, 1998). Turbidites of Norian age in the Trinity Peninsula Group occur near the northern tip of the Antarctic peninsula interbedded with acid volcanic rocks in the Legoupil Formation (Thomson, 1975). Early Triassic turbidites occur in the Myers Bluff Formation of Livingston Island (Willan *et al.*, 1994). Various detrital zircon age population diagrams have been published by Lõske *et al.* (1985) which give strong evidence for Carboniferous and Late Proterozoic source regions.

The confirmation of the Late Triassic depositional age for at least a significant part of the Chonos Metamorphic Complex, implies that its metamorphism took place during the Mesozoic or Cenozoic. However, this metamorphism was probably Jurassic,

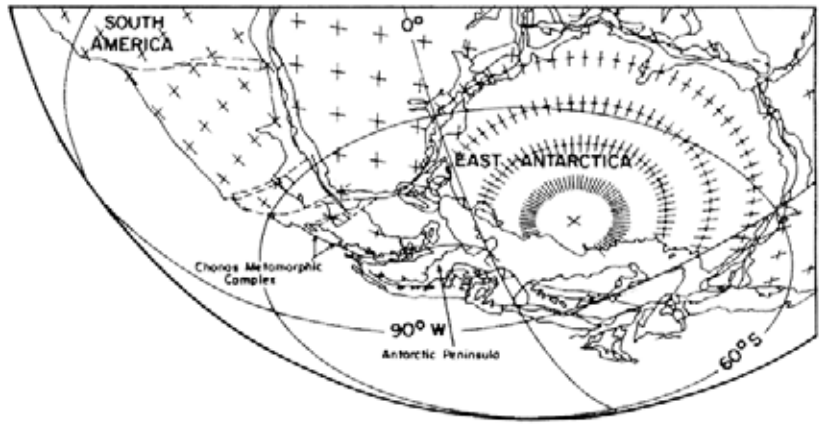

FIG. 4. Part of the tight fit paleogeographic reconstruction of Gondwana at 200 Ma (after Lawver *et al.*, 1998), showing that the present location of the Chonos Metamorphic Complex is just north of the tip of the Antarctic Penisula in the Triassic-Jurassic boundary times.

as the Chonos Metamorphic Complex was intruded by the Early Cretaceous components of the North Patagonian Batholith (Pankhurst *et al.*, 1999), when it had already acquired its main structural charateristics. Also, Thomson *et al.* (2000) combining some of the SHRIMP data presented here and Fission Track age determinations conclude that the metamorphism in the CMC took place in the Early Jurassic. This allows a more confident interpretation of the Late Triassic to Jurassic Rb-Sr age data on rocks of the same unit (*in* Hervé, 1988) as related to the metamorphism or Early diagenesis of the complex.

However, the structurally homogeneous rock units within this metamorphic complex are not necessarily time-restricted depositional units. For example, the metaturbidite from the Teresa facies (Davidson *et al.*, 1987) of the Eastern Belt has given a detrital zircon age spectra which differs from those of the Patranca facies, in that the younger concordant zircon is 336 Ma, and the age *versus* probability pattern is different. They may represent older deposits.

The geographic and lithologic continuity of the Chonos Metamorphic Complex with the Paleozoic Metamorphic Complex of the Coastal Range of southcentral Chile and of the Chiloé island must now be considered carefully. The consequences of the data presented herein lead to significant changes in the interpreted age of deposition and metamorphism of the so-called Paleozoic basement rocks that previously had been considered on the basis of lithological (structural and metamorphic) criteria to form a simple single 'basement' package. Recent work by Duhart *et al.* (1997, 1999); and by Martin *et al.* (1999) in the Lake district of southern Chile, have documented that the Western Series of the paleozoic metamorphic basement includes sedimentary components younger than Early Permian. These same authors indicated that a regional cooling between 220 and 250 Ma is registered in the metamorphic complex, and that it took place after the main deformation and metamorphic event. Söllner *et al.* (2000) reported the presence of Late Carboniferous-Early Permian acid volcanic rocks in the 'basement' near Puerto Montt.

The Late Triassic turbidites of the Chonos Metamorphic complex dated here, are time equivalent to the Panguipulli Formation of the lake district, but the latter, which sits uncomformably over the metamorphic basement, has not experienced the high P/T metamorphism recorded in the CMC. So, the studied rocks were involved in deep subduction during the Late Triassic-Early Jurassic, which took place beneath the western continental margin of Gondwana while the Panguipulli rocks remained on the upper plate near the surface. In the Lake Region, Martin *et al.* (1999) suggested that the Western Series and the Late Carboniferous magmatic arc were exposed after the middle Permian to Middle Triassic exhumation and that initial transpressional deformation of the subduction-arc complex associated with an event of dextral oblique convergence along the margin took place during the Late Triassic-Early Jurassic. This scenario is based on structural observations on the rocks of the Western Series, and on previous paleomagnetic studies (Forsythe *et al.*, 1987) indicating northward translation of portions of the Coast Range, now situated near 30°S during Late Triassic to Late Jurassic. It is interesting to note here that starting in the Early Jurassic, the Antarctic Peninsula migrated southward, with a sinistral movement along the margin of Gondwana after the paleogeographic reconstructions (Scotese, 1997). The Chonos area is thus a portion of the margin where continental margin parallell strike slip movements during the Late Triassic to Early Jurassic seem to diverge, in a way similar to what would be expected when the subduction of a rise or indenter, beneath the continental margin occurs.

The oblique subduction which occurred in the area (Martin *et al.*, 1999) during the Late Triassic-Early Jurassic, together with a low subduction angle, could have resulted in the paucity of the production of magmatic rocks observed during this interval. The most conspicuous contemporaneous arc-like igneous complex is the Sub-cordilleran batholith (Haller *et al.*, 1999) in the eastern slope of the present Andes, which might be genetically related to the subduction event giving rise to the Chonos Metamorphic Complex.

It seems clear that the metamorphic basement of southern Chile certainly includes rocks varying widely in ages of deposition and metamorphism, which otherwise are very similar in structure and metamorphic mineralogy. Precise dating of deposition and metamorphism is a needed basis for understanding its evolution.

ACKNOWLEDGEMENTS

Professor H. Miller (University of München) generously indicated the precise location of the fossil bearing localities he discovered in the 70's, which would have been impossible to relocate otherwise in the maze of islands which compose the Chonos Archipelago. R.J. Pankhurst (British Antarctic Survey), A. Demant (Université d'Aix-Marseille III), A. Willner (Ruhr Universität), H. Massone (Stuttgart Universität), C. Pimpirev (Bulgarian Antarctic Institute) and V. Muñoz (Universidad de Chile) collaborated in the field work. Thorough reviews by H. Miller (München University), M. Martin (Massachussets Institute of Technology) and U. Cordani (Universidad de Sao Paulo) helped to improve the manuscript. This study was funded by Fondecyt Projects 1980741/1010412 and Cátedra Presidencial de Ciencias to FH. It is a contribution to IGCP Project 436 'Pacific Gondwana Margin'.

REFERENCES

Aguirre, L., Hervé, F.; Godoy, E. 1972. Distribution of metamorphic facies in Chile, an outline. *Krystalinikum*, Vol. 9, p. 7-19.

Cingolani, C.; Dalla Salda, L.; Hervé, F.; Munizaga, F.; Pankhurst, R.J.; Parada, M.A.; Rapela, C.W. 1992. Evolution of the North Patagonia Andes and the adjacent continental massif: new impressions of Andean and Pre-Andean Tectonics. *In* Andean Magmatism and its tectonic setting (Harmon, R.; Rapela, C.W.; editors). *Geological Society of America*, Special Paper 265, p. 29-44.

Compston, W.; Williams, I.S.; Kirschvink, J.L.; Zhang Zichau.; Ma Guogan. 1992. Zircon U-Pb ages for the Early Cambrian time-scale. *Journal of the Geological Society of London*, Vol. 149, p. 171-184.

Davidson, J.; Mpodozis, C.; Godoy, E.; Hervé, F.; Pankhurst, R.J.; Brook, M. 1987. Late Paleozoic accretionary complexes on the Gondwana margin of Southern Chile: evidence from the Chonos Archipelago. *In* Gondwana Six: Structure, Tectonics and Geophysics (McKenzie, G.D.: editor). *Geophysical Monograph*, 40, p. 221-227.

Duhart, P.; Martin, M.; Muñoz, J.; Crignola, P.; McDonough, M. 1997. Acerca de la edad del protolito del basamento metamórfico de la Cordillera de la Costa de la X Región. Edades preliminares $^{207}Pb/^{206}Pb$ en circones detríticos. *In Congreso Geológico Chileno, No. 8, Actas*, Vol. 2 p. 1267-1270. Antofagasta.

Duhart, P.; Muñoz, J.; McDonough, M.; Martin, M.; Villeneuve, M. 1999. $^{207}Pb/^{206}Pb$ and $^{40}Ar/^{39}Ar$ geochronology of the coastal metamorphic belt between 41°-42°S in central-south Chile. *In International Symposium on Andean Geodynamics, No. 4, Extended Abstracts Volume*, p. 219-223. Göttingen.

Fang, Z.; Boucot, A.; Covacevich, V.; Hervé, F. 1998. Late Triassic fossils in the Chonos Metamorphic Complex, southern Chile. *Revista Geológica de Chile*, Vol. 25, No. 2, p. 165-173.

Forsythe, R.D.; Kent, D.V.; Mpodozis, C.; Davidson, J. 1987. Paleomagnetism of Permian and Triassic rocks in the central Chilean Andes. *In* Gondwana Six: Structure, Tectonics and Geophysics (McKenzie, G.D.; editor). *Geophysical Monograph*, 40, p. 241-252.

Gradstein, F.; Ogg, J. 1996. A Phanerozoic time scale. *Episodes*, Vol. 19, No. 1-2, p. 3-5.

Haller, M.J.; Linares, E.; Ostera, H.A. 1999. Petrology and geochronology of the subcordilleran plutonic belt of Patagonia. *In South American Symposium on Isotope Geology, No. 2, Actas, Servicio Geológico Minero Argentino, Anales* 34, p. 210-214. Buenos Aires.

Hervé, F. 1988. Late Paleozoic subduction and accretion in Southen Chile. *Episodes*, Vol. 11, p. 183-188.

Hervé, F.; Mpodozis, C.; Davidson, J.; Godoy, E. 1981. Observaciones estructurales y petrográficas en el basamento metamórfico del Archipiélago de los Chonos entre el Canal King y el Canal Ninualac, Aisén. *Revista Geológica de Chile*, No. 13-14, p. 3-16.

Lawver, L.A.; Dalziel, I.W.D.; Gahagan, L.M. 1998. A tight fit Early Mesozoic Gondwana, a plate reconstruction perspective. *Memoirs of the National Institute for Polar Research*, Special issue, Vol. 53, p. 214-229. Tokio.

Löske, W.; Miller, H.; Kramm, U. 1988. U-Pb systematics of detrital zircons from low grade metamorphic sandstones of the Trinity Peninsula Group (Antarctica). *Journal of South American Earth Sciences*, Vol. 1, No. 3, p. 301-307.

Martin, M.; Kato,T.; Rodríguez,C.; Godoy, E.; Duhart, P.; McDonough, M.; Campos, A. 1999. Evolution of Late Paleozoic accretionary complex and overlying forearc-magmatic arc south-central Chile (38-41°S): constraints for the tectonic setting along the south-

western margin of Gondwana. *Tectonics*, Vol. 12, No. 4, p. 582-605.

Miller, H. 1979. Das Grundgebirge der Anden in Chonos-Archipel, Region Aisén, Chile. *Geologische Rundschau*, Vol. 68, No. 2, p. 428-456.

Miller, H.; Sprechmann, P. 1978. Eine devonische Fannula aus dem Chonos-Archipel, Region Aisén, Chile und ihre stratigraphische Bedeutung. *Geologische Jahrbuch*, Vol. B28, p. 37-45.

Paces, J.B.; Miller, J.D. 1993. Precise U-Pb ages of Duluth Complex and related mafic intrusions, northeastern Minnesota: Geochronological insights to physical, petrogenetic, paleomagnetic, and tectonomagmatic process associated with the 1.1 Ga Midcontinent Rift System. *Journal of Geophysical Research*, Vol. 98, No. 13, p. 13997-14013.

Pankhurst, R.J.; Weaver,S.; Hervé, F.; Larrondo, P. 1999. Mesozoic-Cenozoic evolution of the North Patagonian batholith in Aysen, southern Chile. *Journal of the Geological Society of London*, Vol. 156, p. 673-694.

Scotese, C.R. 1997. Continental Drift flip book, 7th edition. Paleomap project. *University of Texas at Arlington, Department of Geology*, 79 p.

Söllner, F.; Alfaro, G.; Miller, H. 2000. A Carboniferous/Permian metaignimbrite from the coastal cordillera west of Puerto Montt, Los Lagos Region, Chile. *In Congreso Geológico Chileno, No. 9, Actas*, Vol. 2, p. 764-768. Puerto Varas.

Manuscript received: September 8, 2000; accepted: June 1, 2001.

Tera, F.; Wasserburg, G. 1972. U-Th-Pb systematics in three Apollo 14 basalts and the problem of initial Pb in lunar rocks. *Earth and Planetary Science Letters*, Vol. 14, p. 281 -304.

Thomson, M.R.A. 1975. New palentological, and lithological observations on the Legoupil Formation, northwest Antarctic Peninsula. *British Antarctic Survey, Bulletin*, No. 41-42, p. 169-185.

Thomson, S.N.; Hervé, F.; Fanning, C.M. 2000. Combining fission-track and U-Pb SHRIMP zircon ages to establish stratigraphic and metamorphic ages in basement sedimentary rocks in southern Chile. *In Congreso Geológico Chileno, No. 9, Actas*, Vol. 2, p. 769-773. Puerto Varas.

Willan, R.C.R.; Pankhurst, R.J.; Hervé, F. 1994. A probable Early Triassic age for the Miers Bluff Formation, Livingston Island, South Shetland Islands. *Antarctic Science*, Vol. 6, No. 3, p. 401-408.

Williams, I.S. 1998. U-Th-Pb geochronology by ion microprobe. *In* Applications of microanalytical techniques to understanding mineralizing processes (McKibben, M.A.; Shanks, W.C.; editors). *Reviews in Economic Geology*, Vol. 7, p. 1 -35.

Willner, A.; Hervé, F.; Massone, H.J. 2000. Mineral chemistry and pressure-temperature evolution of two contrasting high-pressure-low-temperature belts in the Chonos Archipelago, Southern Chile. *Journal of Petrology*, Vol. 41, No. 3, p. 309-330.

TABLE 1. SHRIMP U-Th-Pb RESULTS FOR ZIRCONS FROM SAMPLE CE9603

							Total ratios				Radiogenic Ratios						Ages (Ma) ± error (1 σ)						
Grain. spot	U (ppm)	Th (ppm)	Th/U	Pb*2 (ppm)	$^{204}Pb/^{206}Pb$	f_{204} %	$^{206}Pb/^{238}U$	±	$^{207}Pb/^{206}Pb$	±	$^{206}Pb/^{238}U$	±	$^{207}Pb/^{235}U$	±	$^{207}Pb/^{206}Pb$	±	$^{206}Pb/^{238}U$	±	$^{207}Pb/^{235}U$	±	$^{207}Pb/^{206}Pb$	±	Conc. %
1,1	83	67	0,81	11	0,001712	2,07	16,18	0,51	0,0709	0,0025	0,0605	0,0019					379	12					
2,1	188	488	2,59	20	0,000125	0,17	28,32	0,73	0,0522	0,0015	0,0353	0,0009					223	6					
3,1	436	285	0,65	76	0,000098	0,12	11,78	0,19	0,0587	0,0013	0,0848	0,0014					525	8					
4,1	696	193	0,28	90	0,000448	2,42	14,05	0,23	0,0750	0,0008	0,0694	0,0011					433	7					
5,1	424	181	0,43	36	0,000579	0,48	22,74	0,37	0,0557	0,0011	0,0438	0,0007					276	4					
6,1	91	28	0,30	32	0,000718	1,21	5,36	0,11	0,0885	0,0018	0,1842	0,0040	1,989	0,179	0,0783	0,0068	1090	22	1112	63	1156	178	94
7,1	412	269	0,65	32	0,001033	2,02	25,01	0,43	0,0673	0,0012	0,0392	0,0007					248	4					
8,1	80	30	0,38	28	0,000282	0,48	5,41	0,18	0,0784	0,0017	0,1840	0,0062	1,887	0,112	0,0744	0,0034	1089	34	1077	40	1052	94	103
9,1	163	53	0,33	19	0,000802	0,30	15,74	0,33	0,0571	0,0014	0,0633	0,0013					396	8					
10,1	734	397	0,54	93	0,000277	0,26	15,64	0,28	0,0568	0,0008	0,0638	0,0012					399	7					
11,1	298	226	0,76	53	0,000432	0,38	12,00	0,34	0,0605	0,0021	0,0830	0,0024					514	14					
12,1	230	130	0,56	39	0,000059	0,49	11,74	0,21	0,0617	0,0012	0,0848	0,0015					524	9					
13,1	177	241	1,36	17	0,005195	1,83	25,03	0,57	0,0659	0,0037	0,0392	0,0009					248	6					
14,1	183	238	1,30	16	0,004159	7,50	24,69	0,64	0,1112	0,0032	0,0375	0,0010					237	6					
15,1	645	338	0,52	56	0,000366	0,13	22,87	0,30	0,0529	0,0008	0,0437	0,0006					276	4					
16,1	130	73	0,56	12	0,000530	0,84	21,58	0,47	0,0586	0,0019	0,0460	0,0010					290	6					
17,1	79	25	0,32	13	0,000435	0,68	11,66	0,36	0,0632	0,0033	0,0852	0,0026					527	16					
18,1	662	820	1,24	112	0,000126	0,46	13,66	0,19	0,0597	0,0007	0,0729	0,0010					453	6					
19,1	372	165	0,44	62	0,000079	0,13	11,65	0,16	0,0591	0,0008	0,0858	0,0012					530	7					
20,1	206	55	0,27	24	0,000284	0,19	15,69	0,30	0,0562	0,0012	0,0636	0,0012					398	7					
21,1	196	103	0,52	17	0,002063	4,13	22,48	0,42	0,0847	0,0019	0,0427	0,0008					269	5					
22,1	75	23	0,30	12	0,001498	2,29	11,67	0,25	0,0764	0,0019	0,0837	0,0018					518	11					
23,1	102	95	0,94	14	0,000276	0,78	15,38	0,37	0,0610	0,0033	0,0646	0,0016					404	10					
24,1	63	44	0,70	11	0,000827	1,20	12,45	0,48	0,0657	0,0026	0,0794	0,0031					492	18					
25,1	593	547	0,92	49	0,000010	0,15	25,45	0,42	0,0520	0,0009	0,0378	0,0006					239	4					
26,1	368	133	0,36	67	0,000489	0,53	10,37	0,18	0,0640	0,0009	0,0959	0,0017					590	10					
27,1	714	234	0,33	60	0,001174	0,80	22,67	0,35	0,0583	0,0012	0,0438	0,0007					276	4					
28,1	562	151	0,27	211	0,000058	0,10	4,99	0,07	0,0783	0,0007	0,2002	0,0029	2,139	0,040	0,0775	0,0008	1176	16	1161	13	1134	20	104
29,1	128	51	0,40	17	0,000826	0,35	14,36	0,29	0,0583	0,0032	0,0694	0,0014					433	9					
30,1	171	62	0,36	56	0,000421	0,72	5,86	0,10	0,0794	0,0015	0,1696	0,0030	1,714	0,067	0,0733	0,0024	1010	16	1014	25	1023	67	99
31,1	310	107	0,34	52	0,000769	0,51	11,29	0,25	0,0624	0,0012	0,0881	0,0020					544	12					
32,1	115	159	1,38	9	-	1,66	29,47	0,86	0,0640	0,0035	0,0334	0,0010					212	6					
33,1	138	83	0,60	13	0,000682	0,70	20,85	0,48	0,0580	0,0018	0,0476	0,0011					300	7					
34,1	169	70	0,42	51	0,000211	0,36	6,47	0,13	0,0741	0,0012	0,1539	0,0030	1,508	0,054	0,0711	0,0020	923	17	934	22	959	57	96
35,1	253	54	0,21	27	0,002389	1,18	16,61	0,34	0,0637	0,0024	0,0595	0,0012					373	7					
36,1	111	81	0,73	9	0,003769	4,34	23,52	0,61	0,0861	0,0031	0,0407	0,0011					257	7					
37,1	219	196	0,90	19	0,001762	0,39	25,90	0,45	0,0543	0,0016	0,0385	0,0007					243	4					
38,1	967	352	0,36	79	0,000052	<0,01	23,45	0,29	0,0501	0,0007	0,0427	0,0005					270	3					
39,1	400	202	0,50	126	0,000032	0,06	6,38	0,09	0,0730	0,0012	0,1567	0,0023	1,567	0,039	0,0725	0,0013	938	13	957	15	1001	38	94
40,1	1080	1134	1,05	220	0,000037	0,13	11,13	0,13	0,0596	0,0008	0,0897	0,0010					554	6					
41,1	188	109	0,58	19	0,000149	0,38	19,57	0,47	0,0558	0,0025	0,0509	0,0012					320	7					
42,1	215	68	0,32	31	0,000337	0,04	13,06	0,29	0,0571	0,0013	0,0765	0,0017					475	10					
43,1	652	553	0,85	62	0,000419	0,49	22,65	0,32	0,0558	0,0008	0,0439	0,0006					277	4					
44,1	782	401	0,51	45	0,000964	2,06	33,57	0,51	0,0665	0,0012	0,0292	0,0004					185	3					
45,1	254	87	0,34	32	0,001223	1,52	14,84	0,24	0,0672	0,0013	0,0664	0,0011					414	6					
46,1	486	82	0,17	47	0,000261	1,00	18,40	0,29	0,0616	0,0009	0,0538	0,0008					338	5					
47,1	403	195	0,48	26	0,001158	1,73	29,33	0,59	0,0646	0,0019	0,0335	0,0007					212	4					
48,1	558	25	0,05	76	0,000575	1,02	12,34	0,23	0,0652	0,0009	0,0802	0,0015					498	9					
49,1	71	16	0,22	7	0,012475	7,52	18,16	0,48	0,1132	0,0043	0,0509	0,0014					320	9					
50,1	507	24	0,05	72	-	0,26	12,29	0,18	0,0593	0,0007	0,0811	0,0012					503	7					

Notes 1- uncertainties given at the 1 σ level; 2. f_{204} % denotes the percentage of ^{206}Pb that is common Pb. 3; For areas >800 Ma, correction for common Pb made using the measured $^{204}Pb/^{206}Pb$ ratio. 4. For areas <800 Ma, correction for common Pb made using the measured $^{238}U/^{206}Pb$ and $^{207}Pb/^{206}Pb$ following Tera and Wasserburg (1972) as outlined in Compston *et al.* (1992). 5. For % Conc., 100% denotes a concordant analysis

TABLE 2. SUMMARY OF SHRIMP U-Pb ZIRCON RESULTS FOR SAMPLE FO9606.

							Total ratios				Radiogenic ratios						Age (Ma) ± error (1 σ)						
Grain. spot	U (ppm)	Th (ppm)	Th/U	Pb* (ppm)	$^{204}Pb/^{206}Pb$	f_{206} %	$^{206}Pb/^{238}U$	±	$^{207}Pb/^{204}Pb$	±	$^{206}Pb/^{238}U$	±	$^{207}Pb/^{235}U$	±	$^{207}Pb/^{204}Pb$	±	$^{206}Pb/^{238}U$	±	$^{207}Pb/^{235}U$	±	$^{207}Pb/^{204}Pb$	±	Conc. %
1,1	47	31	0,67	3	0,000136	1,20	23,99	0,72	0,0610	0,0053	0,0412	0,0013					260	8					
2,1	150	108	0,72	28	0,000075	0,08	8,96	0,19	0,0625	0,0010	0,1115	0,0023					682	14					
3,1	137	84	0,61	56	0,000073	0,12	4,08	0,07	0,0882	0,0011	0,2447	0,0041	2,940	0,081	0,0871	0,0017	1411	21	1392	21	1364	39	104
4,1	491	202	0,41	34	0,000010	<0,01	22,63	0,30	0,0519	0,0009	0,0442	0,0006					279	4					
5,1	298	316	1,06	27	0,000100	<0,01	20,60	0,31	0,0519	0,0010	0,0486	0,0007					306	5					
6,1	255	133	0,52	19	0,000355	0,24	21,77	0,34	0,0543	0,0012	0,0458	0,0007					289	4					
7,1	324	180	0,56	23	-	0,14	22,56	0,42	0,0530	0,0011	0,0443	0,0008					279	5					
8,1	284	38	0,13	18	0,000647	0,10	22,31	0,31	0,0527	0,0011	0,0448	0,0006					282	4					
9,1	240	103	0,43	16	0,000100	0,23	23,21	0,48	0,0537	0,0013	0,0430	0,0009					271	5					
10,1	117	82	0,70	9	0,000890	0,27	20,83	0,66	0,0545	0,0027	0,0479	0,0015					302	9					
11,1	199	124	0,62	18	-	0,11	17,70	0,33	0,0546	0,0012	0,0564	0,0011					354	6					
12,1	1549	24	0,02	203	0,000063	<0,01	10,70	0,12	0,0585	0,0005	0,0935	0,0011					576	6					
13,1	129	120	0,93	13	0,000332	0,56	17,03	0,32	0,0583	0,0023	0,0584	0,0011					366	7					
14,1	230	98	0,42	22	-	0,36	16,33	0,32	0,0571	0,0014	0,0610	0,0012					382	7					
15,1	357	219	0,61	27	0,000054	<0,01	21,72	0,35	0,0523	0,0010	0,0461	0,0007					290	5					
16,1	151	144	0,95	9	0,000010	0,17	29,31	0,61	0,0519	0,0030	0,0341	0,0007					216	4					
17,1	81	64	0,80	7	0,002547	0,42	20,49	0,42	0,0560	0,0022	0,0486	0,0010					306	6					
18,1	159	97	0,61	15	0,000375	0,29	17,08	0,29	0,0561	0,0018	0,0584	0,0010					366	6					
19,1	279	100	0,36	20	0,000466	0,04	21,58	0,41	0,0527	0,0011	0,0463	0,0009					292	5					
20,1	109	71	0,65	9	0,000010	0,25	20,27	0,40	0,0545	0,0025	0,0492	0,0010					310	6					
21,1	54	43	0,79	4	0,000326	0,33	22,47	0,57	0,0550	0,0038	0,0444	0,0011					280	7					
22,1	396	135	0,34	28	0,000157	0,17	21,81	0,29	0,0537	0,0009	0,0458	0,0006					289	4					
23,1	825	518	0,63	59	-	0,06	23,00	0,29	0,0523	0,0008	0,0435	0,0006					274	3					
24,1	143	84	0,58	11	0,000152	<0,01	21,52	0,41	0,0522	0,0025	0,0465	0,0009					293	5					
25,1	113	130	1,15	7	-	0,44	30,52	0,82	0,0539	0,0024	0,0326	0,0009					207	6					
26,1	373	27	0,07	30	0,000010	0,15	17,68	0,23	0,0550	0,0009	0,0565	0,0007					354	4					
27,1	191	84	0,44	13	0,000215	0,39	22,78	0,47	0,0550	0,0015	0,0437	0,0009					276	6					
28,1	793	245	0,31	76	0,000077	<0,01	15,75	0,20	0,0544	0,0010	0,0635	0,0008					397	5					
29,1	330	87	0,26	21	0,000005	<0,01	23,50	0,41	0,0514	0,0019	0,0426	0,0008					269	5					
30,1	60	50	0,83	5	0,000010	0,79	20,52	0,48	0,0587	0,0041	0,0484	0,0012					304	7					
31,1	204	76	0,37	17	0,000139	0,09	18,15	0,42	0,0545	0,0014	0,0551	0,0013					345	8					
32,1	232	221	0,95	15	0,000010	<0,01	27,71	0,61	0,0504	0,0015	0,0361	0,0008					229	5					
33,1	386	281	0,73	31	0,000225	<0,01	21,33	0,38	0,0519	0,0015	0,0469	0,0008					295	5					
34,1	1187	24	0,02	154	0,000069	0,13	10,75	0,15	0,0601	0,0005	0,0929	0,0013					573	7					
35,1	368	257	0,70	23	0,000159	<0,01	26,37	0,45	0,0505	0,0018	0,0380	0,0007					240	4					
36,1	709	380	0,54	47	0,000087	0,18	24,06	0,37	0,0529	0,0008	0,0415	0,0006					262	4					
37,1	284	66	0,23	23	-	<0,01	11,09	0,33	0,0570	0,0021	0,0904	0,0027					558	16					
38,1	154	106	0,69	5	0,002090	0,62	29,10	1,13	0,0555	0,0030	0,0342	0,0013					216	8					
39,1	119	19	0,16	12	-	0,46	8,71	0,32	0,0686	0,0023	0,1143	0,0042					697	24					
40,1	241	137	0,57	11	0,000010	0,66	21,70	0,62	0,0574	0,0022	0,0458	0,0013					289	8					
41,1	410	129	0,31	22	-	0,01	17,16	0,39	0,0541	0,0013	0,0583	0,0013					365	8					
42,1	204	78	0,38	8	-	0,06	24,60	0,75	0,0519	0,0027	0,0403	0,0012					255	8					
43,1	177	64	0,36	7	-	0,22	24,30	0,85	0,0532	0,0051	0,0411	0,0015					259	9					
44,1	340	133	0,39	19	0,000258	0,15	16,40	0,41	0,0557	0,0016	0,0609	0,0015					381	9					
45,1	497	228	0,46	20	0,000264	0,01	23,46	0,56	0,0517	0,0018	0,0426	0,0010					269	6					
46,1	622	497	0,80	68	0,000121	0,78	9,41	0,18	0,0674	0,0015	0,1054	0,0020					646	12					
47,1	530	133	0,25	19	-	0,50	24,27	0,46	0,0554	0,0022	0,0410	0,0008					259	5					
48,1	172	72	0,42	6	0,001841	0,41	26,07	0,66	0,0547	0,0025	0,0382	0,0010					242	6					
49,1	77	63	0,82	3	0,003858	0,74	29,10	1,17	0,0565	0,0066	0,0341	0,0014					216	9					
50,1	969	55	0,06	134	0,000010	0,02	6,16	0,09	0,0746	0,0007	0,1623	0,0024	1,667	0,031	0,0745	0,0007	970	14	996	12	1055	19	92
51,1	86	75	0,88	16	0,000115	0,20	5,73	0,19	0,0780	0,0022	0,1740	0,0057	1,832	0,092	0,0763	0,0026	1034	31	1057	34	1104	70	94
52,1	67	39	0,58	3	-	0,75	21,51	0,97	0,0585	0,0035	0,0461	0,0021					291	13					
53,1	426	91	0,21	17	-	<0,01	22,42	0,56	0,0511	0,0016	0,0447	0,0011					282	7					
54,1	238	210	0,88	13	0,000461	0,04	18,50	0,61	0,0541	0,0019	0,0540	0,0018					339	11					
55,1	605	42	0,07	29	0,000010	<0,01	17,28	0,43	0,0536	0,0012	0,0579	0,0014					363	9					
56,1	205	143	0,70	16	-	0,54	12,65	0,45	0,0614	0,0020	0,0786	0,0028					488	17					
57,1	174	107	0,61	13	-	0,09	12,89	0,43	0,0577	0,0017	0,0775	0,0026					481	15					
58,1	106	33	0,31	4	0,002113	0,84	22,65	0,95	0,0586	0,0032	0,0438	0,0019					276	11					
59,1	484	247	0,51	34	-	<0,01	13,48	0,34	0,0556	0,0016	-0,0742	0,0019					462	11					
60,1	244	114	0,47	10	0,000268	0,41	22,95	0,60	0,0551	0,0018	0,0434	0,0011					274	7					

Notes. 1- uncertainties given at the 1 σ level. 2- f_{206} % denotes the percentage of ^{206}Pb that is common Pb; 3- for areas >800 Ma, correction for common Pb made using the measured $^{204}Pb/^{206}Pb$ ratio; 4- for areas <800 Ma, correction for common Pb made using the measured $^{207}U/^{206}Pb$ and $^{207}Pb/^{206}Pb$ following Tera and Wasserburg (1972) as outlined in Compston *et al.* (1992); 5. For % Conc., 100% denotes a concordant analysis

TABLE 3. SUMMARY OF SHRIMP U-Pb ZIRCON RESULTS FOR SAMPLE CE9625.

							Total ratios				Radiogenic ratios					Age (Ma) ± error (1 σ)						
Grain. spot	U (ppm)	Th (ppm)	Th/U	Pb* (ppm)	$^{204}Pb/^{206}Pb$	f_{206} %	$^{206}Pb/^{238}U$	±	$^{207}Pb/^{206}Pb$	±	$^{206}Pb/^{238}U$	±	$^{207}Pb/^{235}U$	±	$^{207}Pb/^{206}Pb$	±	$^{206}Pb/^{238}U$	±	$^{207}Pb/^{235}U$	±	$^{207}Pb/^{206}Pb$	±	Conc. %
1,1	680	331	0,49	55	0,000309	0,40	13,55	0,81	0,0595	0,0012	0,0735	0,0044					457	27					
2,1	155	52	0,34	9	0,001318	2,35	17,43	0,63	0,0726	0,0020	0,0560	0,0020					351	12					
3,1	317	212	0,67	18	-	1,53	20,31	0,43	0,0646	0,0026	0,0485	0,0010					305	6					
4,1	65	30	0,46	3	0,007027	17,20	17,25	0,91	0,1922	0,0328	0,0480	0,0035					302	21					
5,1	367	174	0,47	42	0,000154	1,26	9,45	0,19	0,0716	0,0011	0,1045	0,0021					641	12					
6,1	407	201	0,49	21	0,001052	1,85	21,44	0,36	0,0671	0,0029	0,0458	0,0008					289	5					
7,1	241	39	0,16	11	0,002525	4,20	21,36	0,64	0,0860	0,0024	0,0449	0,0014					283	8					
8,1	66	52	0,79	4	0,004030	12,25	17,77	1,07	0,1523	0,0080	0,0494	0,0030					311	19					
9,1	94	28	0,30	18	0,000049	<0,01	5,84	0,16	0,0936	0,0032	0,1712	0,0048	2,193	0,104	0,0929	0,0033	1019	26	1179	34	1465	68	69
10,1	80	46	0,60	5	0,001652	3,96	19,04	0,65	0,0848	0,0032	0,0504	0,0018					317	11					
11,1	397	156	0,39	21	0,000491	0,80	20,61	0,48	0,0588	0,0019	0,0481	0,0011					303	7					
12,1	331	161	0,49	17	0,001428	2,12	21,36	0,53	0,0693	0,0021	0,0458	0,0011					289	7					
13,1	167	72	0,43	8	0,001607	4,26	20,84	0,65	0,0865	0,0038	0,0459	0,0015					290	9					
14,1	138	134	0,97	11	0,001987	2,26	15,05	0,56	0,0732	0,0023	0,0650	0,0024					406	15					
15,1	165	140	0,85	7	0,000197	0,61	30,24	0,66	0,0552	0,0026	0,0329	0,0007					208	5					
15,2	185	128	0,69	10	0,000326	0,99	28,45	0,50	0,0585	0,0013	0,0348	0,0006					221	4					
16,1	821	224	0,27	55	0,000001	0,23	17,19	0,20	0,0556	0,0011	0,0580	0,0007					364	4					
17,1	333	131	0,39	18	0,000292	1,58	21,68	0,39	0,0648	0,0013	0,0454	0,0008					286	5					
18,1	614	461	0,75	36	0,000172	0,51	22,56	0,27	0,0560	0,0008	0,0441	0,0005					278	3					
19,1	115	111	0,96	39	-	<0,01	4,23	0,07	0,0881	0,0013	0,2364	0,0039	2,880	0,068	0,0884	0,0013	1368	21	1377	18	1391	29	98
20,1	328	29	0,09	201	0,000049	0,08	2,00	0,03	0,1804	0,0010	0,5003	0,0065	12,400	0,185	0,1798	0,0010	2615	28	2635	14	2651	10	99
21,1	123	94	0,76	5	0,002367	2,89	29,16	0,58	0,0734	0,0029	0,0333	0,0007					211	4					
21,2	153	189	1,24	9	0,000679	1,97	29,74	0,51	0,0661	0,0024	0,0330	0,0006					209	4					
22,1	446	133	0,30	32	0,000282	0,43	16,08	0,24	0,0579	0,0012	0,0619	0,0009					387	6					
23,1	762	208	0,27	55	0,000026	0,23	15,97	0,19	0,0563	0,0012	0,0625	0,0007					391	4					
24,1	211	176	0,83	17	0,000256	0,81	19,49	0,26	0,0593	0,0025	0,0509	0,0007					320	5					
25,1	172	127	0,74	25	0,000422	0,51	10,87	0,16	0,0629	0,0010	0,0915	0,0014					565	8					
26,1	64	28	0,44	19	0,000128	0,13	5,07	0,09	0,0804	0,0016	0,1967	0,0035	2,132	0,063	0,0786	0,0017	1157	19	1159	21	1163	44	100
27,1	49	28	0,58	4	0,004250	2,37	17,19	0,39	0,0729	0,0041	0,0568	0,0013					356	8					
28,1	259	48	0,19	121	0,000014	<0,01	3,20	0,06	0,1641	0,0025	0,3125	0,0057	7,063	0,179	0,1639	0,0025	1753	28	2119	23	2496	26	70
29,1	113	84	0,75	17	0,000349	0,67	10,77	0,22	0,0643	0,0016	0,0922	0,0019					569	11					
30,1	297	258	0,87	17	0,000390	0,54	27,38	0,38	0,0550	0,0013	0,0363	0,0005					230	3					
31,1	302	140	0,46	20	0,000387	0,62	22,21	0,34	0,0568	0,0011	0,0448	0,0007					282	4					
32,1	115	81	0,71	11	0,000010	0,51	16,11	0,38	0,0583	0,0023	0,0618	0,0015					386	9					
33,1	196	105	0,53	47	0,000010	0,01	6,39	0,10	0,0744	0,0008	0,1565	0,0025	1,603	0,032	0,0743	0,0008	937	14	971	13	1049	21	89
34,1	636	95	0,15	72	0,000074	<0,01	11,97	0,17	0,0578	0,0006	0,0836	0,0012					517	7					
35,1	184	68	0,37	23	0,000129	4,67	10,59	0,17	0,0969	0,0019	0,0900	0,0015					555	9					
36,1	479	223	0,47	32	0,000165	0,38	21,87	0,34	0,0550	0,0008	0,0456	0,0007					287	4					
37,1	252	272	1,08	16	0,000254	0,77	27,52	0,45	0,0569	0,0012	0,0361	0,0006					228	4					
38,1	115	97	0,84	37	0,000238	0,41	5,08	0,09	0,0816	0,0010	0,1961	0,0034	2,115	0,067	0,0782	0,0019	1154	18	1154	22	1153	50	100
39,1	43	6	0,15	2	0,004525	3,83	22,66	0,82	0,0823	0,0039	0,0425	0,0015					268	10					
40,1	51	15	0,30	4	0,001992	1,77	18,50	0,45	0,0672	0,0043	0,0531	0,0014					333	8					
41,1	85	54	0,63	8	0,002080	0,68	15,74	0,39	0,0602	0,0016	0,0631	0,0016					395	10					
42,1	301	96	0,32	20	0,000224	0,76	20,92	0,30	0,0584	0,0010	0,0475	0,0007					299	4					
43,1	238	72	0,30	16	0,000464	0,69	20,50	0,41	0,0579	0,0011	0,0485	0,0010					305	6					
44,1	750	286	0,38	49	0,000159	0,30	21,84	0,26	0,0544	0,0006	0,0456	0,0006					288	3					
45,1	390	201	0,51	28	0,000001	0,16	20,85	0,31	0,0536	0,0010	0,0479	0,0007					302	4					
46,1	245	127	0,52	21	0,000377	0,54	17,32	0,27	0,0581	0,0013	0,0574	0,0009					360	6					
47,1	393	526	1,34	37	0,000268	<0,01	19,10	0,25	0,0526	0,0011	0,0524	0,0008					329	5					
48,1	354	209	0,59	28	0,000190	0,25	18,99	0,31	0,0550	0,0010	0,0525	0,0009					330	5					

Notes. **1-** uncertainties given at the 1 σ level; **2-** f_{206} % denotes the percentage of ^{206}Pb that is common Pb; **3-** for areas >800 Ma, correction for common Pb made using the measured $^{204}Pb/^{206}Pb$ ratio; **4-** for areas <800 Ma, correction for common Pb made using the measured $^{238}U/^{206}Pb$ and $^{207}Pb/^{206}Pb$ following Tera and Wasserburg (1972) as outlined in Compston *et al.* (1992); **5-** for % Conc., 100% denotes a concordant analysis.

TABLE 4. SUMMARY OF SHRIMP U-Pb ZIRCON RESULTS FOR SAMPLE FO9640.

							Radiogenic ratios						Ages (Ma) ± error (1 σ)						
Grain. spot	U (ppm)	Th (ppm)	Th/U	Pb* (ppm)	$^{204}Pb/^{206}Pb$	f_{206} %	$^{206}Pb/^{238}U$	±	$^{207}Pb/^{235}U$	±	$^{208}Pb/^{206}Pb$	±	$^{206}Pb/^{238}U$	±	$^{207}Pb/^{235}U$	±	$^{207}Pb/^{206}Pb$	±	Conc. %
1,1	76	59	0,78	15	0,000103	0,23	0,1164	0,0025					710	15					
2,1	489	48	0,10	128	0,000002	<0,01	0,1600	0,0024	1,844	0,032	0,0743	0,0007	1067	13	1061	11	1049	19	102
3,1	1324	30	0,02	265	0,000000	<0,01	0,1415	0,0017					853	10					
4,1	436	379	0,87	43	-	0,25	0,0570	0,0009					357	6					
5,1	358	116	0,32	213	0,000032	0,05	0,3724	0,0046	6,429	0,098	0,1252	0,0010	2041	22	2036	14	2032	14	100
6,1	160	260	1,63	26	0,000243	0,06	0,0788	0,0014					489	8					
7,1	210	102	0,49	129	0,000020	0,03	0,3737	0,0064	5,882	0,194	0,1142	0,0030	2047	30	1959	29	1867	48	110
8,1	297	203	0,68	82	0,000077	0,13	0,1630	0,0025	1,628	0,041	0,0724	0,0013	973	14	981	16	998	37	98
9,1	159	262	1,64	123	0,000072	0,11	0,3687	0,0078	6,090	0,143	0,1198	0,0010	2023	37	1989	21	1953	14	104
10,1	116	40	0,35	34	-	<0,01	0,1899	0,0031	1,970	0,072	0,0752	0,0023	1121	17	1105	25	1075	63	104
11,1	1217	63	0,05	186	0,000064	0,50	0,1091	0,0012					667	7					
12,1	749	90	0,12	126	0,000035	<0,01	0,1164	0,0014					710	8					
13,1	436	614	1,41	66	0,000082	0,03	0,0777	0,0010					482	6					
14,1	120	107	0,89	23	0,000446	0,10	0,1097	0,0019					671	11					
15,1	260	168	0,60	34	0,000199	0,21	0,0742	0,0013					461	8					
16,1	269	44	0,16	73	-	<0,01	0,1838	0,0038	1,827	0,078	0,0721	0,0025	1087	21	1055	29	989	73	110
17,1	241	105	0,44	68	0,000037	0,06	0,1783	0,0031	1,783	0,041	0,0725	0,0010	1058	17	1039	15	1000	27	106
18,1	134	17	0,13	20	0,005754	11,75	0,1086	0,0023					665	14					
19,1	97	33	0,34	13	-	0,32	0,0876	0,0022					541	13					
20,1	85	38	0,45	54	0,000166	0,25	0,3874	0,0069	6,825	0,180	0,1278	0,0022	2111	32	2089	24	2068	31	102
21,1	223	324	1,45	39	0,000217	0,31	0,0894	0,0016					552	9					
22,1	46	35	0,77	11	0,002882	2,30	0,1467	0,0047					883	27					
23,1	776	329	0,42	158	0,000010	0,30	0,1309	0,0017					793	10					
24,1	1135	545	0,48	314	0,000032	0,05	0,1719	0,0019	1,761	0,023	0,0743	0,0004	1023	10	1031	8	1050	11	97
25,1	113	106	0,94	18	0,000578	0,22	0,0873	0,0023					540	14					
26,1	230	65	0,28	69	0,000023	0,04	0,1937	0,0029	2,170	0,044	0,0812	0,0010	1142	16	1171	14	1227	23	93
27,1	430	451	1,05	44	0,000065	<0,01	0,0573	0,0008					359	5					
28,1	224	66	0,29	45	0,000320	0,15	0,1328	0,0021					804	12					
29,1	766	459	0,60	113	0,000010	0,01	0,0898	0,0015					555	9					
30,1	125	55	0,44	25	0,000054	1,14	0,1244	0,0024					756	14					
31,1	156	163	1,05	31	0,000201	0,27	0,1097	0,0025					671	15					
32,1	482	391	0,81	63	0,000010	<0,01	0,0754	0,0010					469	6					
33,1	445	44	0,10	53	0,000031	<0,01	0,0831	0,0011					514	7					
34,1	311	110	0,35	87	0,000010	0,02	0,1801	0,0026	1,834	0,040	0,0738	0,0011	1068	14	1058	14	1037	30	103
35,1	281	158	0,56	24	-	<0,01	0,0535	0,0008					336	5					
36,1	282	20	0,07	38	0,000006	0,28	0,0959	0,0013					590	8					
37,1	348	198	0,57	33	0,000188	0,45	0,0582	0,0009					365	6					
38,1	110	44	0,40	53	0,000113	0,18	0,3024	0,0051	4,546	0,105	0,1090	0,0015	1703	25	1739	19	1783	25	96
39,1	125	50	0,40	34	0,000252	0,43	0,1722	0,0036	1,736	0,068	0,0731	0,0022	1024	20	1022	26	1018	63	101
40,1	152	99	0,65	49	-	<0,01	0,1903	0,0029	2,041	0,125	0,0778	0,0045	1123	15	1129	43	1141	119	99
41,1	157	35	0,23	25	0,000297	0,10	0,1066	0,0025					653	14					
42,1	91	75	0,82	108	0,000044	0,06	0,6242	0,0119	19,32	0,40	0,2245	0,0015	3127	47	3058	20	3013	11	104
43,1	356	157	0,44	65	0,000029	<0,01	0,1153	0,0017					704	10					
44,1	208	119	0,57	31	-	<0,01	0,0903	0,0015					557	9					
45,1	215	98	0,45	73	0,000073	0,12	0,2116	0,0036	2,400	0,065	0,0823	0,0016	1237	19	1243	20	1252	38	99
46,1	648	306	0,47	59	0,000139	0,12	0,0576	0,0007					362	4					
47,1	548	62	0,11	68	0,000003	<0,01	0,0868	0,0011					537	6					
48,1	158	70	0,45	41	0,000039	0,07	0,1634	0,0027	1,631	0,043	0,0724	0,0014	976	15	982	17	997	38	98
49,1	120	67	0,56	100	0,000161	0,22	0,4779	0,0105	11,29	0,28	0,1713	0,0017	2518	45	2547	24	2570	17	98
50,1	352	156	0,44	60	0,000019	0,08	0,1077	0,0018					660	10					
51,1	311	246	0,79	31	0,000024	0,59	0,0972	0,0019					598	11					
52,1	647	229	0,35	56	0,000010	0,02	0,0953	0,0015					587	9					
53,1	567	264	0,47	51	0,000082	0,22	0,0956	0,0016					589	10					
54,1	347	141	0,41	28	-	0,32	0,0876	0,0017					541	10					
55,1	314	160	0,51	47	0,000112	0,21	0,1588	0,0031	1,611	0,047	0,0736	0,0014	950	17	975	18	1030	40	92

Notes: **1-** uncertainties given at the 1 σ level; **2-** f_{206} % denotes the percentage of ^{206}Pb that is common Pb; **3-** for areas >800 Ma, correction for common Pb made using the measured $^{207}Pb/^{204}Pb$ ratio; **4-** for areas <800 Ma, correction for common Pb made using the measured $^{238}U/^{204}Pb$ and $^{207}Pb/^{206}Pb$ following Tera and Wasserburg (1972) as outlined in Compston *et al.* (1992); **5-** for % Conc., 100% denotes a concordant analysis.